DEEP-LEARNING BASED IDENTIFICATION OF INDUCER CAVITATION INSTABILITY

Youngkuk Yoon
Seoul National University
truesky1218@snu.ac.kr

Sang Hyeon Lee
Seoul National University
bear11235@snu.ac.kr

Seung Jin Song
Seoul National University
sjsong@snu.ac.kr

ABSTRACT

A deep-learning based method is introduced to detect and identify the inducer cavitation instability. To identify alternate blade cavitation, which is a common cavitation instability occurs at two-bladed inducer, synthetic unsteady pressure data under equal length cavitation and alternate blade cavitation have been generated and used as training data sets. The neural network is trained to categorize the unknown unsteady pressure signal into with or without cavitation instability. In the present research, the network shows good performance in capturing the key features of the instability and robustness against random noise compared with the previous mode analysis technique

INTRODUCTION

Inducer cavitation instabilities manifest themselves as various frequency peaks located above and below the shaft frequency harmonics with certain spatial mode and propagating direction. As the operating condition, such as flow coefficient and cavitation number, changes and the number of inducer blades varies, different types of cavitation instability occur. For instance, alternate blade cavitation, under which large and small cavity are developed at the inducer blades in alternating sequence, only occurs at even-number-bladed inducer [1].

To identify those cavitation instabilities, unsteady pressure measurements at the inducer inlet have been widely used [2]. Through Fourier transformation of the unsteady pressure time series obtained from the single pressure transducer, various frequency peaks can be identified, and various cavitation instabilities can be categorized. Furthermore, to determine the spatial mode (also called as cell number) and propagating direction, multiple pressure transducers can be used simultaneously. For example, if two unsteady pressure transducers are installed at the same axial position while 90 degree apart circumferentially, the cell number and the propagating direction of the instability can be speculated by comparing the phase of the Fourier coefficients whose frequencies are the peak frequencies. Generally, to completely determine the cavitation instability characteristics, 2n+1 unsteady pressure transducer should be installed circumferentially due to the Nyquist-Shannon sampling theorem, where n is the spatial mode of the cavitation instability of interest. While typical cavitation instabilities are composed of less than three cells, five pressure transducers could be installed to fully identify the cavitation instability.

To determine the frequency, spatial mode, and propagating direction from the multiple unsteady pressure time signals, Traveling Wave Energy (TWE) method is often used [3]. TWE method, which could be simply explained as double Fourier transformation in time and space, firstly conducts Fourier transformation which converts time domain into frequency domain. Then, the Fourier coefficients of the peak frequencies from the multiple unsteady pressure measurements are again Fourier transformed, spatial domain into spatial mode (also can be interpreted as a spatial frequency) domain. Hence, TWE method uses the spatial information (circumferentially installed position) of the unsteady pressure transducers to determine the governing spatial mode for each peak frequency. Using TWE method, characteristic frequency, spatial mode, and propagating direction of the cavitation instability can be obtained at once.

However, while the mathematical rigorous and low computational cost of the TWE method are based on the orthogonality of the harmonic functions, instalment of the unsteady pressure transducer with unequal circumferential spacing could undermine the advantages of the TWE method. For example, in many inducer experiments, visualization of the cavity is needed to identify the cavity structure. Thus, at least half of the casing circumference should be cleared for the camera access. Then, the unsteady pressure transducers could be only installed at some limited region of the circumference, and the circumferential distance between adjacent transducers would not be uniform. Also, practical issues such as transducer wires could cause non-uniform distribution of the transducers [4]. In such case, matrix inversion is needed to obtain the magnitude of each spatial mode for the specific frequency. Because of the high conditional number of the matrix, especially with non-uniformly installed pressure transducers, slight noise of the phase and magnitude of the frequency component for each unsteady pressure time series can induce

highly erroneous results. Furthermore, if the unsteady flow phenomena contain higher spatial mode than the maximum possible spatial mode (n) which can be resolved using the given amount of unsteady pressure time series, decomposition into various spatial modes can be even unrealistic. For instance, even though the inducer only suffers from the super-synchronous rotating instability, which is a single-cell instability, O(1) percent of error in Fourier coefficient from unsteady time series could make the zeroth spatial mode most prominent, and then the instability would identified as a global instability such as surge, which can be simply refuted via cavity visualization.

Therefore, the present paper suggests deep-learning based method to identify the inducer cavitation instability to utilise raw unsteady pressure time series directly. Thus, cavitation instabilities can be recognized as certain collective pattern in the high-dimensional raw data. Also, while the present method proposes effective data reduction and feature extraction method for the periodical high-dimensional data, it serves as a framework for the neural network for the general turbomachinery experimental data, and auto-detection and auto-classification of the instability, including previously unknown ones.

MODEL DESCRIPTION

To successfully capture the characteristic features of the complex high-dimensional data, kernel-type data process is included in the present convolution neural network. While the general fully connected neural networks are not adequate to abstract features from the periodical data, kernel layer, which is widely used in reducing high-dimensional flow field [7, 8], should be added to pre-process the raw data and reduce it to a low-dimensional space. The basic operation principle of the kernel layer is shown in Fig. 1. In the present neural network, kernels do not slide through the raw data one data entity at a time, but jump multiple data entities to effectively reduce the dimension of the raw data.

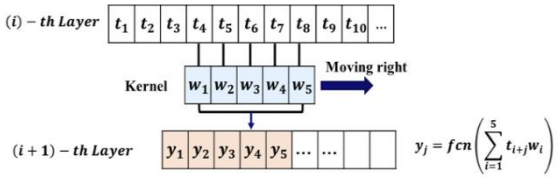

Fig. 1. Schematic diagram of the kernel layer

In the present study, identifying inducer cavitation instability of the two-bladed inducer is simulated. For a given flow coefficient, the same extent of cavity is developed for the both blades of the inducer due to the axisymmetricity under sufficiently high inlet pressure. However, as the inducer inlet pressure decreases and the system becomes susceptible to the cavitation, large extent of cavitation develops and alternate blade cavitation usually occurs. Under alternate blade cavitation, cavity pattern is fixed under the rotating frame. However, both blades have different cavity extent. On one blade, longer cavity is developed and shorter cavity is developed on the other blade. In this case, the force is exerted to the axis as if the inducer is imbalanced, and asymmetricity occurs. The purpose of the study is to discriminate the equal length cavity situation and the alternate blade cavitation only by directly using the raw data. Thus, synthetic data for the unsteady pressure measurements were generated for the equal length cavity and alternate blade cavitation cases. Under equal length cavity situation, due to the symmetricity, the only frequency component which is excited is the blade passing frequency (2 times shaft rotating frequency). Therefore, if the forward direction is defined as the rotating direction of the inducer, equal length cavity situation would show blade passing frequency, two cells, and forward propagating characteristic. To reconstruct this characteristic as the unsteady pressure signal, inverse Fourier transformation is done with relative random noise (relative magnitude of the Fourier coefficient with respect to the magnitude of blade passing frequency) of 1% for all frequencies but the peak frequency. Also, to simulate the realistic experimental condition, five pressure transducers were supposed to installed in the inducer inlet with the circumferential position of 0, 90, 135, 180, and 270 degree. To implement the possible manufacturing and measurement error, the mounting position of the pressure transducers are also varied randomly with in ±1 degree. Typical synthetic unsteady pressure signal from a single pressure transducer is shown in Fig. 2.

On contrary, due to the asymmetricity of the alternate blade cavitation, not only blade passing frequency component, shaft rotating frequency is also excited. Thus, shaft rotating frequency, single cell, forward propagating instability is added to the equal length cavity baseline case. The relative magnitude of the Fourier coefficient for the shaft rotating frequency is defined as A.B.C. strength in the present paper.

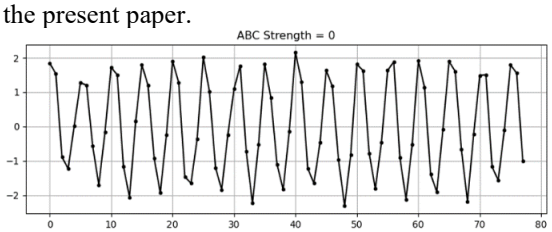

Fig. 2. Typical synthetic unsteady pressure signal under equal length cavity

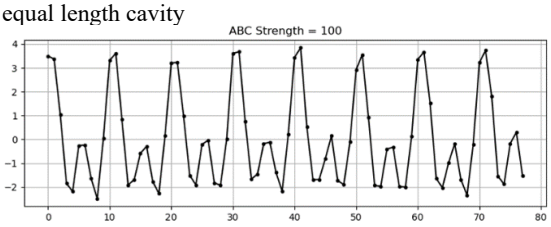

Fig. 3. Typical synthetic unsteady pressure signal under alternate blade cavitation

The random noises and errors for the other frequency components and transducer mounting positions are set the same as the equal length cavity case. Typical synthetic unsteady pressure signal under alternate blade cavitation with A.B.C. strength of 100% is shown in Fig. 3

To extract the relevant features from the given synthetic raw data, the following method was used. First, auto-encoder structure is used to extract the key feature from the raw data. Both encoder and decoder are composed of three stages. 4th encoder stage was only used for the classification procedure, which will be explained later. Figs. 4 and 5 show the schematic diagram of the encoder and the decoder.

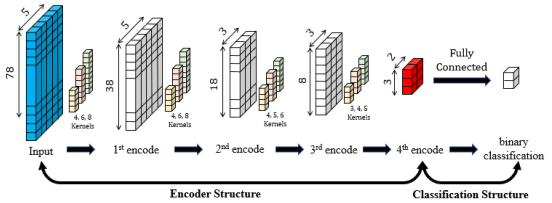

Fig. 4. Schematic diagram of the encoder

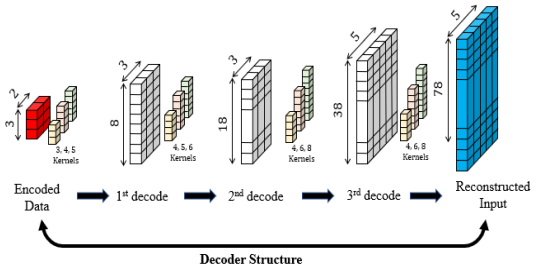

Fig. 5. Schematic diagram of the decoder

The encoder-decoder set is trained in stack. The first stage encoder is directly connected to the first stage decoder and trained to minimize the difference between input raw data and the reconstructed input data. Then, the second stage encoder which is followed by the second stage decoder is connected to the already-optimized first stage encoder. This second stage encoder-decoder pair is trained to minimize error between the first encoded data and the corresponding reconstructed data. Third stage encoder-decoder pair is also trained in the same way. These training processes are shown schematically in Figs. 6-8.

Second, to examine the encoder whether it can automatically extract the features which serve as criteria for the instability detection, the raw data is connected to the kernel layer which is followed by the encoder. The fourth stage encoder reduces the high-dimensional data into a low-dimensional data of 2 by 3, which further reduces the dimension to make ease of the classification. Then, the encoder is connected to the binary node layer for the classification between equal length cavity and alternate blade cavitation. A.B.C. strength of 0% and 10% are used as train data corresponding to the equal length cavity, and A.B.C. strength of 90% and 100% are used as alternate blade cavitation case.

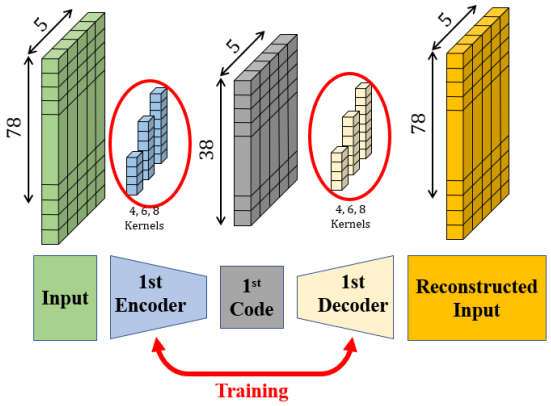

Fig. 6. Schematic diagram of the first stage encoder-decoder pair

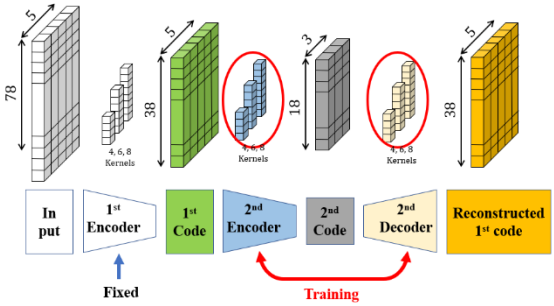

Fig. 7. Schematic diagram of the second stage encoder-decoder pair

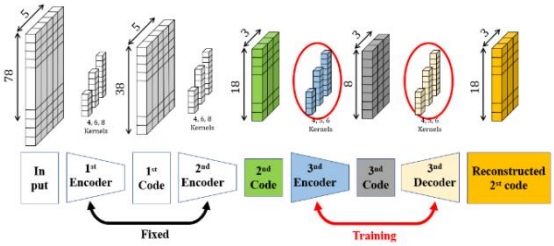

Fig. 8. Schematic diagram of the third stage encoder-decoder pair

After the training, test data (randomly selected from 0 to 100% A.B.C. strength) were examined whether or not it is correctly categorized to equal cavity length case and alternate blade cavitation

RESULTS AND DISCUSSIONS

Firstly, the encoder-decoder pair is tested whether it can adequately represent the raw input data by only using low-dimensional data whose dimension is nearly 20 times reduced. Fig. 9 shows the coded data for the two training cases, A.B.C. strength of 0% and 100%, after fourth encoder, which is compressed into 6-dimensional data. The abscissa of the graph shows the reduced dimension, which corresponds to each node, and the ordinate shows the value of the nodes. A band-type data, which is plotted on the graph, is due to the small discrepancies among the trained data caused by the presence of the noise. The narrow band shows that even though some degree of noise was imposed to the training data, key features of the data are well

captured, and the features are barely susceptible to the noise. Although the physical meaning of each reduced dimension can hardly be known, two distinct forms of the data between A.B.C. strength of 0% and 100% shows that different pattern between those two cases are properly captured.

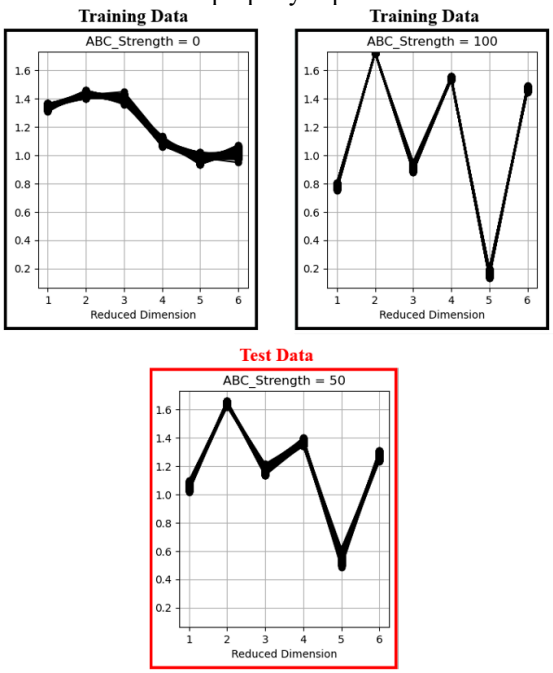

Fig. 9. Compressed low-dimensional data

The coded data shown in Fig. 9 are recovered by the decoder, which is trained along with the encoder. Fig. 10 shows the comparison between input data and the reconstructed data via the decoder. As shown in Fig. 10, both A.B.C. strength of 0% and 100% data are almost fully recovered and their dominant features are maintained after the reconstruction from the low-dimensional compressed data. Therefore, with the selection of the appropriate kernel layers, quasi--periodic high-dimensional unsteady data can be compressed into the low-dimensional data without the loss in key features.

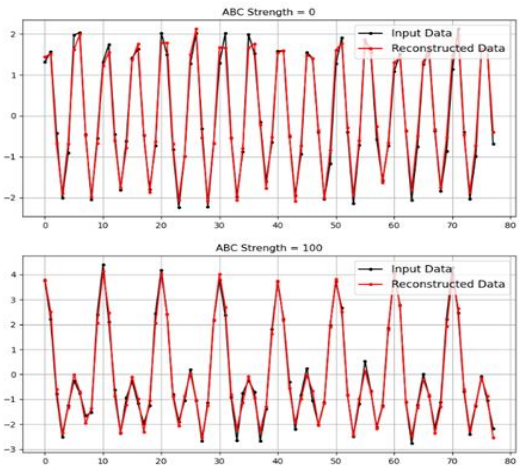

Fig. 10. Comparison between the input data and the reconstructed data

After verifying the encoder-decoder system and the validation of the compressed data, training data were categorized under supervision with two groups: equal length cavity and alternate blade cavitation. Categorization module consists of two nodes, whose state represent the group to which the input data will be allocated. For example, [1 0] state corresponds to the perfect equal length cavity case (A.B.C. strength of 0% without noise), and [0 1] state corresponds to the perfect alternate blade cavitation case (A.B.C. strength of 100% without noise). Even though the values of the nodes do not have to be the probabilities, the values can be interpreted as a probability, by which an input data belongs to a certain group, at least in the present research while they are programmed to satisfy the mathematical definition of the probability. After the training, test data, including the A.B.C. strength other than 0% and 100%, were also put into the categorization module to verify whether the key features of the alternate blade cavitation compared to equal length cavity were correctly captured. If the key features are well captured, as the A.B.C. strength increases monotonically, the probability for the A.B.C. should have to also increase monotonically. If the network is overfitted or the categorization module exploited some minor features to differentiate equal length cavity and alternate blade cavitation, the untrained data will be categorized randomly, without coherent trend (at least in human eye). The values of the second node (representing A.B.C. group) for the randomly selected untrained data can be shown in Fig. 11.

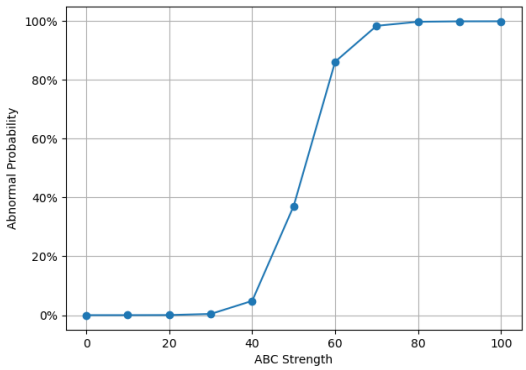

Fig. 11. Alternate blade cavitation probability for the various untrained data sets

As shown in Fig. 11, although the test data with A.B.C. strength between 10 to 90% have not been used for the training, as the A.B.C. strength increases, A.B.C. probability also monotonically increases. Therefore, it can be said that the present neural network captures the key features of the unsteady pressure measurement under A.B.C. in good accordance with the traditional instability criteria. Also, the sigmoidal form of the above probability graph suggests that the present neural network also has the practical advantage for the instability identification (categorization) problems.

To test the applicability of the neural network beyond the training data in the manner of extrapolation, training data sets were set as the A.B.C. strength of 0 and 50%. All the other schemes including the encoder-decoder training were the same with the 0 & 100% training data case. In 0 & 50% case, not only the in-between values (which can be considered as an interpolation problem), 60 to 100% of the A.B.C. strengths were tested. If the present neural network categorizes the equal blade cavity and the alternate blade cavity based on specific values of the 50% A.B.C. strength case, and not based on the general key features of the alternate blade cavitation (overfitted), the extrapolation beyond 50% A.B.C. strength will fail, and their probability will have the value other than 1. However, Fig. 12 shows that this is not the case. Fig. 12 shows the probability graph for A.B.C. strength of 0 to 100%, which is obtained with the training data of 0 and 50% A.B.C. strength. From the Fig. 12, it can be shown that the A.B.C. values larger than 60% are all identified as alternate blade cavitation. Hence, once the key features of the instability are determined, the present neural network shows the good performance for the instability detection regardless of its magnitude.

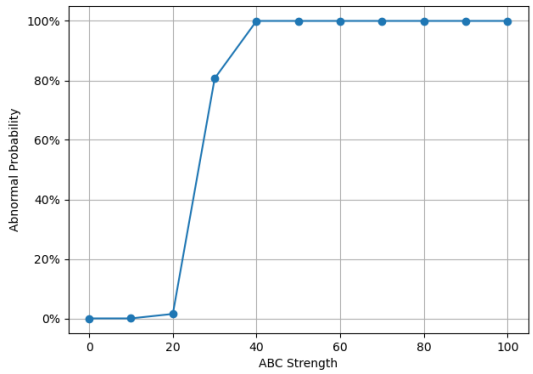

Fig. 12. Alternate blade cavitation probability for the various untrained data sets (trained by 0 and 50% A.B.C.)

The practicality of the present neural network approach can be much emphasized in comparison with the previous Fourier-transformation-type detection methods, especially when the pressure transducers should be placed in the limited area. These situations often occur in turbomachinery measurements, due to the practical considerations. For instance, in case of making both flow field visualization and pressure measurements available, the transducer should be installed in the limited area due to provide optical access through the casing. To mimic those situations, the synthetic data were newly generated, assuming that each of the measurements were conducted at 0, 36, 72, 108, and 144 degrees (restricted to the half-annulus). As before, the data contains random noise in the Fourier coefficient itself, and installed positions are also assumed to be subjected to random Gaussian error, to include the possible manufacturing tolerance. In the case of the neural network approach, change in measurement positions hardly affects the results. Alternate blade cavitation is well identified and similar results with Figs. 11 and 12 are obtained. To compare with the present method, Traveling Wave Energy (TWE) method [5] was selected for the Fourier-transformation-type instability detection scheme. It is based on the double Fourier transformation in time and space domain, which can obtain the frequency, spatial mode (up to second mode with five measurement points, following Nyquist-Shannon sampling theorem), and propagating direction. To briefly explain, the pressure signals are first decomposed into various spatial modes as follows [3]:

$$g(t,\theta) = Re\left\{\sum_{n=0}^{N}\begin{pmatrix}\delta g_{nR}(t) - \\ j\cdot\delta g_{nI}(t)\end{pmatrix}\cdot e^{jn\theta}\right\} \qquad (1)$$

Then, the obtained spatial Fourier coefficients, $\delta g_{nR}(t)$ and $\delta g_{nI}(t)$, are temporally Fourier transformed to obtain $e^{j(n\theta-\omega t)}$ (forward propagating) and $e^{j(n\theta+\omega t)}$ (backward propagating) components. Thus, the raw unsteady pressure signal would be decomposed into various propagating canonical modes, and by interrogating the dominant modes, the presense of the instability can be said.

However, even though TWE method gives much information about the instabillity, it can be prone to the noise if the measurement stations are not distributed unifomly around the circumference. With the present assmption of compact unsteady pressure transducer install area, the condition number of the inverse spatial Fourier transformation matrix (by which $\delta g_{nR}(t)$ and $\delta g_{nI}(t)$ can be obtained with Eq. (1)) is larger than 40. Therefore, small error could cause the significant error in signal decomposition. For example, even though the difference in A.B.C. strength for each measurement location is less than 5%, and the phase error between two adjacent stations is less than 5 degrees (which is a typical error level in the experiment), 100% A.B.C. strengh would be judeged as containing surge (0^{th} spatial mode instability) with almost 56% relative magnitude (Table 1). This can be emphasized by plotting the complex temporal Fourier coefficient of the blade passing frequency compared with the from the five measurement stations, compared with the values for the noiseless alternate blade cavitation. In Fig. 13, five dots shows the temporal Fourier coefficient of the synthetic data with noise. Also shown in Fig. 13 as the orange lines are the 0, 36, 72, 108, and 144 degrees angle line. If there are no noises and only signal of 100% A.B.C. strength is added to the equal cavity length case, all of the Fourier coefficients should exist at the intersection between the orange lines and the unit circle. It can be seen that the actual deviation between the noise contained synthetic data and the noiseless case is almost negligible. However, it results in significant

error in instability detection while Fourier-transformation-type scheme is used.

Therefore, if the main purpose of the expeirment is identification and categorization of the instability, especially when each instaiblity has distinctive feature and its occurence realm hardly overlaps, the present method provide more robustness against the noise and practical limitations. Although both neural network approach and Forier-transformation-type approach are mathematically rigorous, the concepts of the approach are different, and the neural network could have much values in certain situation as mentioned above (of course, in other situations, Fourier-transformation-type approach could be more appropriate). In case of the Fourier transformation, the decomposition of raw signal into modes are performed with fixed set of orthogonal functions, namely, harmonic functions. If multiple instabilities occur simultaneously, mode decomposition with Fourier transformation is useful to distinguish all the instabilities.

Table 1. Mode decomposition of the synthetic data with the restricted area of unsteady pressure measurements

Instability type	**Relative magnitude (as defined in the same way with the A.B.C. strength)**
Backward propagating 2nd spatial mode	19.63%
Backward propagating, 1st spatial mode	44.15%
0th spatial mode (surge-type)	56.00%
Forward propagating, 1st spatial mode	79.99%
Forward propagating, 2nd spatial mode	15.00%

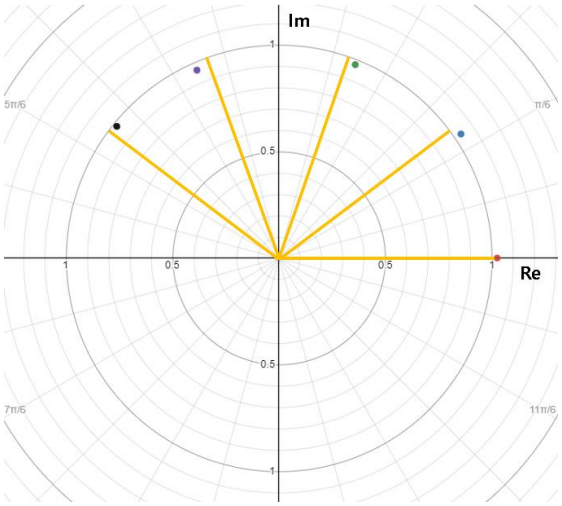

Fig. 13. Temporal Fourier transformation coefficients from five measurement stations in restricted area case

However, as in many turbomachinery applications, if each instability mode appears distinctly and even suppresses other modes (such as compresssor stall and surge [6]), rather than mode decomposition using the fixed set of orthogonal function, finding appropriate set of orthogonal functions that each of them could robustly represent corresponding instability is of much interest. In such case, the neural network approach is more pertinent for the purpose due to its feature extracting capability.

As a demonstration of the simple supervised binary categorization for the high-dimensional quasi-periodic data, the present research serves as a framework for the categorization of multiple instabilities. Also, by introducing the unsupervised auto-clustering technique to the present resarch, previously unlearned instability can be captured, which would show unexpected patterns or features in the raw signals, and might be used to detect hardly discernible instability precursors, including compressor pre-stall behaviors.

SUMMARY AND CONCLUSIONS

The new conclusions from this study are as follows

- A new method based on the neural network which could directly extract key features from the high-dimensional quasi-periodic raw data, and robustly identify the cavitation instability has been developed.
- The data has been compressed into low-dimensional data which can almost fully represent the original high-dimensionality. This has been done through the encoder strucutre and the kernel layer. The data compression precedure has been verified using the encoder-decoder pair, which has been trained together in stack.
- The present method provides more robust instability identification schemes against noise compared to the Fourier-transformation-type scheme. Also, the key feature extracting capability of the present scheme can be used for the general multi-instability categorization and capturing pre-instability behavior.

ACKNOWLEDGMENTS

This work was supported by the National Research Foundation of Korea (NRF) grant funded by the Korea government (MSIT) (No. 2021R1A2C2014609). Financial support from the BK21+ Program and Institute for Advanced Machinery and Design (SNU-IAMD) is also gratefully acknowledged by the authors.

REFERENCES

1. J.-D. Huang, M. Aoki, J.-T. Zhang, JSME Int. J. Ser. B **41**, 1 (1998)
2. Y. Tsujimoto, Y. Yoshida, Y. Maekawa, S. Watanabe, T. Hashimoto, J. Fluids Eng. **119**, 4 (1997)

3. C. Lettieri, Z. Spakovszky, D. Jackson, J. Schwille, J. Propuls. Power **34**, 2 (2018)
4. Y. Yoon, J. Kim, S. J. Song, Exp. Therm. Fluid Sci. **132** (2022)
5. M. Tryfonidis, O. Etchevers, J. D. Paduano, A.H. Epstein, G. J. Hendricks, J. Turbomach. **117**, 1 (1995)
6. F. K. Moore, E. M. Greitzer, J. Eng. Gas Turbines Power, **108**, 1 (1986)
7. T. Nakamura, K. Fukami, K. Hasegawa, Y. Nabae, K. Fukagata, Phys. Fluids, **33**, 2 (2021)
8. K. Hasegawa, K. Fukami, T. Murata, K. Fukagata, Theor. Comput. Fluid Dyn., **34**, 4 (2020)